plasma

MDPI

Article

Plasma Treatment of Different Biodegradable Polymers: A Method to Enhance Wettability and Adhesion Properties for Use in Industrial Packaging

Espedito Vassallo [1,*], Matteo Pedroni [1], Marco Aloisio [1], Silvia Maria Pietralunga [2,3], Riccardo Donnini [4], Francesca Saitta [5] and Dimitrios Fessas [5]

1 Institute for Plasma Science and Technology (ISTP), National Research Council (CNR), Via R. Cozzi 53, 20125 Milan, Italy; matteo.pedroni@istp.cnr.it (M.P.); marcoaloisio1996@gmail.com (M.A.)
2 Institute for Photonics and Nanotechnologies (IFN), National Research Council (CNR), p.zza Leonardo da Vinci 32, 20133 Milan, Italy; silviamaria.pietralunga@cnr.it
3 Center for Nano Science and Technology @PoliMi, Istituto Italiano di Tecnologia, Via Rubattino, 81, 20134 Milan, Italy
4 Institute of Condensed Matter Chemistry and Technologies for Energy (ICMATE), National Research Council (CNR), Via R. Cozzi 53, 20125 Milan, Italy; riccardo.donnini@cnr.it
5 Department of Food, Environmental and Nutritional Sciences (DeFENS), Università degli Studi di Milano, Via Celoria 2, 20133 Milan, Italy; francesca.saitta@unimi.it (F.S.); dimitrios.fessas@unimi.it (D.F.)
* Correspondence: espedito.vassalllo@cnr.it

Abstract: Biodegradable polymers (poly(butylene succinate (PBS)), poly(butylene adipate terephthalate (PBAT)) and poly(lactic acid)/poly(butylene adipate terephthalate (PLA/PBAT)) blend) were treated in radiofrequency (13.56 MHz) low-pressure (10 Pa) oxygen with argon post-crosslinking plasma to enhance wettability and adhesion properties. Surface morphology and roughness modification caused by plasma exposure were observed by scanning electron microscopy (SEM) and atomic force microscopy (AFM). Surface chemical modifications of plasma-treated samples were evaluated by Fourier Transform infrared spectroscopy (FTIR). Due to the limited durability of plasma activation, the hydrophobic recovery was evaluated by water contact angle (WCA) measurements. The ageing effect was measured over 15 days in order to assess this kind of treatment as a potential industrial scalable method to increase biodegradable polymers *hydrophilic* properties for food packaging applications. The effects of polymer activation on its weight loss were also determined. Differential scanning calorimetry (DSC) analysis was used to study the effect of plasma treatment on the thermal properties of the polymers, while the crystallinity was investigated by X-ray diffraction (XRD).

Keywords: poly(butylene succinate); poly(butylene adipate terephthalate); wettability; ageing; plasma treatment; surface modification

Citation: Vassallo, E.; Pedroni, M.; Aloisio, M.; Pietralunga, S.M.; Donnini, R.; Saitta, F.; Fessas, D. Plasma Treatment of Different Biodegradable Polymers: A Method to Enhance Wettability and Adhesion Properties for Use in Industrial Packaging. *Plasma* **2024**, *7*, 91–105. https://doi.org/10.3390/plasma7010007

Academic Editors: Carles Corbella and Andrey Starikovskiy

Received: 17 November 2023
Revised: 19 January 2024
Accepted: 23 January 2024
Published: 26 January 2024

1. Introduction

Despite the numerous advantages that polymer offers in the food packaging field due to its excellent performance in terms of flexibility, being lightweight and having low production costs [1], its petroleum nature and its difficult disposal make this material a danger to human health and the environmental ecosystem [2]. From this point of view, the use of more sustainable materials seems to be increasingly necessary. Biodegradable polymers (BPs) are known to be environmentally benign materials since they are biocompostable, accessible, stable, non-toxic and inexpensive materials. Their eco-friendly attributes combined with excellent mechanical properties make BPs a valid alternative to the most used commercial plastics in the food packaging field [3]. Moreover, BP films share a common feature with traditional packaging polymer films: they are hydrophobic surfaces and are typically characterized as low surface energy materials. However, this behavior limits their ability to adhere to other material layers, their ability to be sealed and their

printability characteristic [4] and this inhibits their intended wide range of applications. Surface treatment is a commonly used method to improve these drawbacks, giving short and long-term effects on the polymer according to the desired application and leaving unchanged the bulk material properties [5]. Wet chemical treatment is a well-used method to increase the surface energy of the most common traditional plastics through a reaction between a sample and a specific solvent [6–8]. Unfortunately, it requires additional steps during the process such as rinsing, washing and drying and this drastically increases the amount of waste generated during each operation. Plasma treatment, being a simple, clean, solvent-free and fast process, represents a valid eco-friendly alternative to change polymer surface wettability, printability and adhesion properties [9]. In addition, the possibility of creating a non-equilibrium plasma (or cold plasma) provides low-temperature treatments, making this method particularly suitable for polymer substrates [10]. When a plasma is generated by exposing a gaseous mixture to a high electric field, the energetic particles, radicals or photons produced may react with the polymer surface. This interaction can lead to the cleavage of polymer chains, resulting in the breaking of chemical bonds within the polymer structure. The outcome may involve either the scission of the polymer chain in shorter fragments, facilitated by sufficiently high energy, or the crosslinking of the polymer, inducing the formation of chemical bonds between different polymer chains and altering the polymer network structure. Furthermore, depending on the reactive plasma species, specific functional groups can be introduced into the polymer chain, thereby inducing modifications in the surface properties of the polymer [11]. Different gaseous mixtures could create different functional groups, depending on the desired application. For example, it is well known that oxygen-based plasma introduces various functional groups such as hydroxyl, carboxyl and carbonyl groups that increase the hydrophilicity of polymeric substrates [12]. For all of these mentioned reasons, plasma activation has been extensively analyzed in the scientific literature to treat conventional polymeric substrates such as polyethylene terephthalate (PET) [13], low-density polyethylene (LDPE) [14], polypropylene (PP) [15] and polystyrene (PS) [16]. However, there are few studies about these surface treatments on BPs in the scientific literature, most of which concern biomedical and tissue engineering applications [17–21] or the study of the superhydrophilicity of polymeric nanofibrous membranes during plasma exposure [22]. Our work is focused on the investigation of plasma activation of three different BP substrates used in the food packaging field: two promising materials such as poly(butylene adipate terephthalate) (PBAT) and poly(butylene succinate) (PBS) which are considered a good alternative to commercial plastics for the package design of wraps or bags [23] and a BP blend composed of 60% PBAT and 40% poly(lactic acid) (PLA) which, exploiting the properties of the two constituent polymers, has been used to enhance the antibacterial activity of fruit packages [24]. As the activation process causes an increase in the surface energy of the sample, there is a fast rearrangement of the polar functional groups to decrease and minimize this energy surplus, which corresponds to a hydrophobic recovery of the treated surface (ageing phenomenon) [25]. For these reasons, plasma activation durability is a very important industrial scale-up issue. In order to reduce the ageing of the activated surfaces, the substrates pre-treated with oxygen plasma can be exposed to an argon mixture which produces a crosslinked layer on a polymer surface and impedes the movement of functional groups [26]. Thus, the investigated BP substrates were exposed to an oxygen plasma followed by an Ar one. The two-step process is schematically illustrated in Figure 1b,c, respectively. This work aims to evaluate the effect of this plasma activation treatment (process parameters have been previously optimized and described in [27]) on the BP surfaces just mentioned. Morphological properties of pristine and treated films were investigated through SEM and AFM. Chemical surface information about untreated and plasma-activated BPs was obtained by FTIR characterization. The samples' wettability during their storage was evaluated using optical contact angle (OCA) measurements and the ageing phenomenon was evaluated during a 15-day post-treatment period. Finally, the materials' bulk properties in terms of thermal behavior and crystallinity were investigated before and after the plasma treatments through DSC and XRD, respectively.

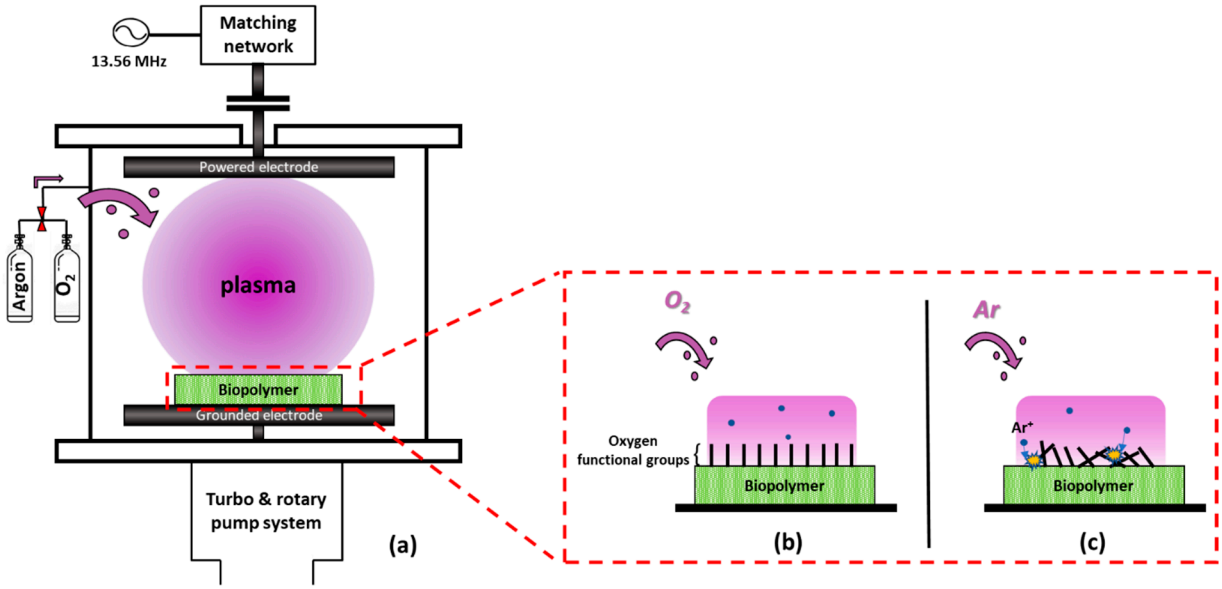

Figure 1. Experimental set up used. (**a**) Oxygen (**b**) and argon post-crosslinking (**c**) surface modification mechanism.

2. Experimental Section

2.1. Materials

Investigations were evaluated using samples of PBS foil (BioPBS™ FZ91PM/FZ91PB, Bangkok, Thailand, thickness 30 µm), PBAT (BIO TH801T, Chemdo Shanghai, China, thickness 20 µm) and PLA/PBAT 40/60 (Biofilm 3055 LR, IMB Roma Italy, thickness 20 µm) of 4 × 4 cm^2 size. Before plasma treatments, BPs were cleaned by filtered air for 1 min at room temperature. All samples were stored at room temperature and 40% relative humidity. Oxygen (99.998% purity) and argon (99.999% purity) gases were Rivoira products.

2.2. Process Reactor and Plasma Parameters

The experimental setup consists of a capacitively coupled plasma-enhanced chemical vapor deposition (PECVD) system with a cylindrical stainless steel vacuum chamber of 25 cm inner diameter, characterized by an asymmetric parallel-electrode configuration (Figure 1a) [28]. The plasma is formed by means of a radiofrequency (RF) ($\omega_{rf}/2\pi$ = 13.56 MHz) supplied by a Hüttinger generator (model PFG 300 RF) with a matching box (model PFM 1500 A). The operating pressure is maintained constant (10 Pa) through a pumping system made by a turbo pump (TURBOVAC 150 L/s, Leybold), backed by a rotary pump (TRIVAC 24 m^3/h, Leybold). During both activation processes, a constant flow rate was used and the operating gas pressure was controlled by adjusting the mass flow controller (MSK Flow) and measured by a capacitive vacuum gauge. Samples are treated first with 30 s oxygen and immediately after with 1 min or 2 min argon plasma with an RF power input value of 100 W (power density 0.3 W/cm^2). Table 1 reports some macroscopic experimental parameters of the processes and plasma parameters, such as plasma density (n_e) and electron temperature (T_e), estimated by an rf compensated Langmuir probe (LP). It consists of a tungsten tip with a 0.1 mm diameter and a length of 15 mm. The current–voltage (*I*–*V*) curves were acquired by applying ±40 V on the LP. Plasma parameters were extracted from ten scans and averaged for the operation of each *I*–*V* curve through the semi-automatics data analysis mode. The probe tip was cleaned after each measurement (30 V was applied to the probe for an exposure time of 100 ms).

For a probe in the orbital motion limited (OML) regime [29] and assuming a Maxwellian distribution, the average T_e was determined as T_e (eV) = 1/slope of the plot of natural logarithm of the *I*–*V* curve of the probe in the region between the floating potential (*Vf*) and plasma potential (*Vp*), while the n_e was calculated from the electron current saturation

region [30,31]. Samples were placed on the lower electrode which is grounded (connected to the chamber wall) and is spaced 8.5 cm from the powered electrode. The LP was positioned 2 cm from the grounded electrode. In order to evaluate the thermal load caused by the plasma process, the specimen temperature was monitored by a thermocouple (K type) fixed close to (0.01 m) the sample itself.

Table 1. Experimental conditions of plasma treatments.

Plasma Gas	Total Gas Flow (Sccm)	Electron Density (m^{-3})	Electron Temperature (eV)	Self-Bias Voltage V_{dc} (V)
Oxygen plasma	20	$2 \times 10^{14} \pm 10\%$	1 ± 0.1	−450
Ar post-crosslinking plasma	20	$2.5 \times 10^{15} \pm 10\%$	1.7 ± 0.1	−440

2.3. Weight Loss Measurements

The etching effect with plasma was monitored by measuring the weight loss of the polymer samples. The samples were weighed just before being mounted into the plasma reactor, and then again just after the plasma treatment. A Sartorius Secura® (Sartorius, Göttingen, Germany) professional microbalance was used. The accuracy of the measurements is, according to the producer, 0.01 mg.

2.4. Surface Characterization

Chemical characterization of the plasma-treated BPs was performed using a Perkin Elmer Spectrum Two FT-IR spectrometer equipped with an Attenuated Total Reflection (ATR) accessory, in which air was used as a background and all spectra were recorded from 650 to 4000 cm^{-1} with a resolution of 4 cm^{-1}, averaging 20 scans for each measurement. The ATR accessory has a diamond crystal of refractive index 2.4 at 1000 cm^{-1} with a depth penetration [32] of about 1.8 μm at a 45° angle of incidence (using a substrate mean refractive index of 1.45). For each sample, an averaged FTIR spectrum through five different surface areas was reported. The topography and roughness of the samples were analyzed by atomic force microscopy in dynamic mode (CoreAFM, Nanosurf GmbH, Langen, Germany). The AFM images were post-processed with Gwyddion software. The roughness of each sample was obtained (before and after plasma exposure) by analyzing 5 different portions of the surface and averaging the roughness values obtained. The images were collected at a size of 10 × 10 μm^2. High-resolution scanning electron microscope (Hi-res SEM, Tescan mod. MIRA III) imaging was used to evaluate the morphology of films, both at the surface and in the cross-section. For accurate SEM imaging, samples were metalized by depositing an ultra-thin layer of gold (about 8 nm) through sputtering in order to provide an electrical discharge path. High-resolution SEM images at the surface were taken at 30 keV of electron beam energies and 10 keV was used for cross-section images while optimizing for beam current and pixel dwell time to avoid film damage while maximizing the contrast.

2.5. X-ray Diffraction (XRD) and Differential Scanning Calorimetry (DSC) Analysis

The bulk characterization was performed for treated samples (PBS, PBAT and PLA/PBAT) in O_2 plasma for 30 s with Ar post-crosslinking of 1 min. Possible changes in the crystallinity state were investigated by an X-ray diffractometer with Bragg–Brentano geometry and copper Kα radiation. The X-ray diffraction data were collected in the 2θ range from 10° to 70° with a step size of 0.05° and a velocity of 5 s/step. DSC analysis was performed to measure the thermal properties of PBS, PBAT and the PLA/PBAT blend samples. Both untreated and plasma-treated materials (over 15 days of ageing) were investigated by using a DSC 2920 (TA Instrument, New Castle, DE, USA) calorimeter with stainless steel sealed pans (10 mg samples). The first heating scan from 20 °C to 200 °C at 5 °C·min^{-1} was considered. An empty pan was used as reference and calibration was carried out with indium as standard. Data analysis was performed with the dedicated software IFESTOS following procedures reported in previous studies [33]. In brief, the

output signal in mW units was normalized by the mass of each sample and multiplied by the inverse of the scanning rate to obtain the apparent specific heat thermogram C_P ^{app} (T)/J·K^{-1}·g^{-1}. Successively, the baseline extrapolated from the late part of the thermograms (i.e., after any visible peak), which represent the polymer in the molten state, was subtracted to obtain the excess specific heat C_P ^{exc} (T)/J·K^{-1}·g^{-1}. Three replicates were performed for each system.

2.6. Water Contact Angle Measurements

The analyses of the contact angle were performed using an FKV (Bergamo, Italy) DataPhysics OCA20 goniometer. The surface wettability was obtained using the value of the contact angle obtained with a 4 µL drop of distilled water dropped on the surface of the samples with a 500 µL Hamilton syringe. The variations in the surface wettability were studied for 15 days. At least 3 to 4 replicate measurements were executed for each sample and a mean value was reported.

3. Results and Discussion

3.1. Morphological Changes Induced by Plasma

AFM images (Figure 2) were used to evaluate any topographical changes in BP surfaces caused by plasma treatment (see Section 2.2). In the pristine state, PBS and the PLA/PBAT blend were characterized by a uniform fibrillar morphology, while in the PBAT film, there were a few valleys in a more disordered structure.

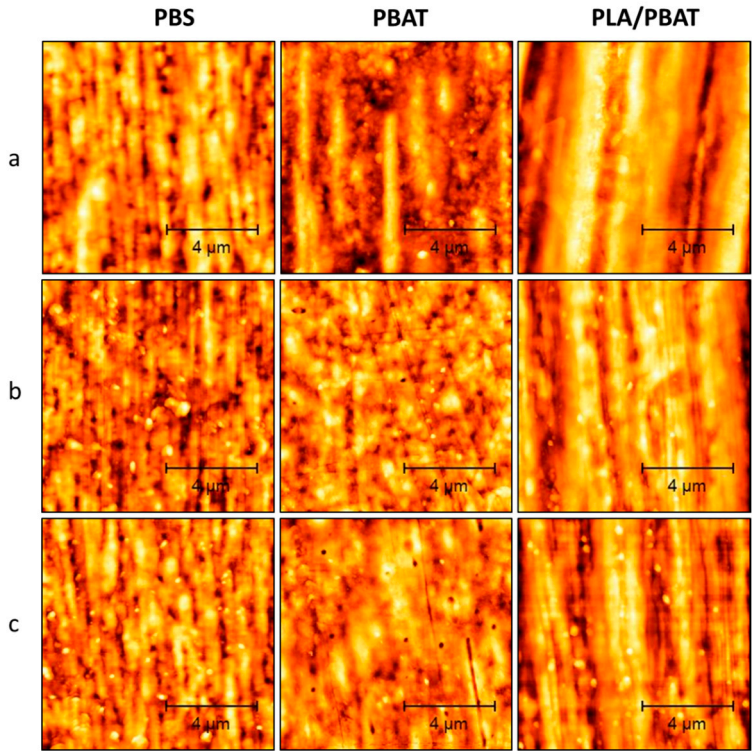

Figure 2. AFM images of PBS, PBAT and PLA/PBAT blend in their untreated state (**a**) and treated with 1 min (**b**) and 2 min (**c**) Ar post-crosslinking process.

It was found that the surface roughness R_a was not significantly modified by the plasma treatment for PBS, while more pronounced variations were noted in the case of the other two treated polymers, particularly with regard to the PBAT/PLA blend (R_a values are summarized in Table 2). This can be ascribed to the distinct crystalline structure of the polymers (see Section 3.4). The higher crystallinity and, hence hardness of PBS, would account for the slight morphological changes observed, especially when compared to the other two polymers subjected to identical treatment conditions.

Table 2. Average roughness values of untreated and plasma-treated samples.

Biopolymer	Untreated	Crosslinked 1 min	Crosslinked 2 min
PBS	26.5 ± 4.4	24.6 ± 2.9	23.9 ± 4
PBAT	22.6 ± 1.3	19.8 ± 4.1	16.6 ± 2.8
PLA/PBAT	105.5 ± 13.5	63 ± 10.2	66.5 ± 10.8

Average roughness, R_a [nm].

On the other hand, the PLA/PBAT blend surface was characterized by nanosized structures and smoother profiles, with the R_a value reduced by about 60% already after 1 min of Ar crosslinking plasma treatment. This topographical change could be partially attributable to the effect of argon particles sputtering after the oxygen etching process [34]. Moreover, we assume that this degradation effect could be associated with the synergy of the interaction of plasma particles with the surface chemical bonds and the simultaneous rise in temperature due to ion bombardment. Indeed, this could lead to surface temperatures above 60 °C, and as the blend material at such temperatures is already above the glass transition temperature ascribable to PLA fraction [35], the high mobility of the material surface molecules may justify the strong reduction in R_a. Thermal load measurements during the plasma process support what has just been said, as the temperature recorded at the end of the process was in the range of 50–60 °C. The SEM characterization confirms the variations in the morphological features of the raw materials treated by plasma. In particular, as for the PBAT and PLA/PBAT samples, the 2 min Ar process (Figure 3c) seems to change the morphological properties, causing the formation of surface defects (some of these denoted by red arrows) on the materials. These results show that only a 1 min Ar process does not produce morphological damage on substrate surfaces, highlighting how previously optimized plasma parameters are not invasive for this kind of polymer but only change the surface properties [27].

3.2. Weight Loss by Plasma Etching

During the oxygen plasma activation of polymers, the surface layer is functionalized (polar groups) and, at the same time, is etched by plasma particles. The weight loss due to etching was therefore analyzed. The etching rate (R_{et}, mg/cm^2 min) was calculated from the ratio between the weight loss and the oxygen plasma exposure time. R_{et} was very low for PBS at around 0.028 mg/cm^2 min, while for PBAT and the PLA/PBAT blend, the value was around 0.048 mg/cm^2 min. These data are also consistent with the crystalline structures of the treated polymers. Specifically, the polymer exhibiting a lower etching rate is the most crystalline, namely, PBS. Regarding the next process with argon (crosslinking), R_{et} was also evaluated at around 0.004 mg/cm^2 min for PBS and 0.006 mg/cm^2 min for PBAT and the PLA/PBAT blend. However, these R_{et} are acceptable values for a possible industrial application, also in light of the fact that the processing time was optimized to one and a half minutes.

3.3. Stability of Surface-Treated BP Films: Ageing Phenomenon

The surface wettability over time of plasma-treated BPs was evaluated from the measurements of the water drop contact angle for 15 days (400 h) after the activation process. As shown (Figure 4), every sample became super hydrophilic immediately after plasma exposure, with a WCA value of less than 3°, highlighting how this treatment causes polar groups' functionalization on the BP surfaces. Moreover, over the storage time, a synergic process consisting of a rearrangement of functional groups in order to minimize surface energy and a passivation process due to exposure to air causes hydrophobic recovery, and hence, an intense WCA value increase was observed [36]. During the first 48 h of ageing, the increase in WCA is most pronounced compared to the next 350 ageing hours. Considering the WCA values for the native samples (continuous and black line in the graphs) and the values of treated samples after 400 h of ageing time, a decrease in the WCA value of about 23%, 38% and 22% is evidenced for PBS, PBAT and the PLA/PBAT blend, respectively. The

difference between the value obtained for PBAT and that of the other two treated polymers does not have a straightforward and immediate explanation. In fact, the hydrophilic ageing of a plasma-treated polymer is closely tied to changes in its structure induced by the plasma treatment. However, different aspects must be considered regarding the relationship between the hydrophilic ageing of a plasma-treated polymer and its structure. These include polymer molecular weight, abundance of chemical functional groups, surface morphology and crystallinity. Thus, an in-depth comprehension of the evolving structural changes induced by plasma treatment, their temporal progression and their interconnections is necessary for prediction of the long-term behavior of the treated polymers. Regardless, the obtained results show that the oxygen plasma with Ar post-crosslinking activation improves, even after 400 h, surface hydrophilic properties compared to the untreated BP behavior, highlighting how this kind of process is an important industrial scale-up issue for improving BP wettability and adhesion in industrial packaging applications. Just to make a comparison, the WCA trend in pure oxygen plasma-treated BPs without post-crosslinking was also inserted. These ageing experiments clearly show that even 2 days after this treatment, BP samples still have considerably higher hydrophilicity than the untreated sample. The figure also shows that very similar results were obtained between the 1 min (dotted black curve) and 2 min (dotted red curve) crosslinking treatment. In light of the results obtained, the appropriate processing time (also taking into account a possible technology transfer to industry) was fixed at 30 s for O_2 plasma with Ar post-crosslinking of 1 min.

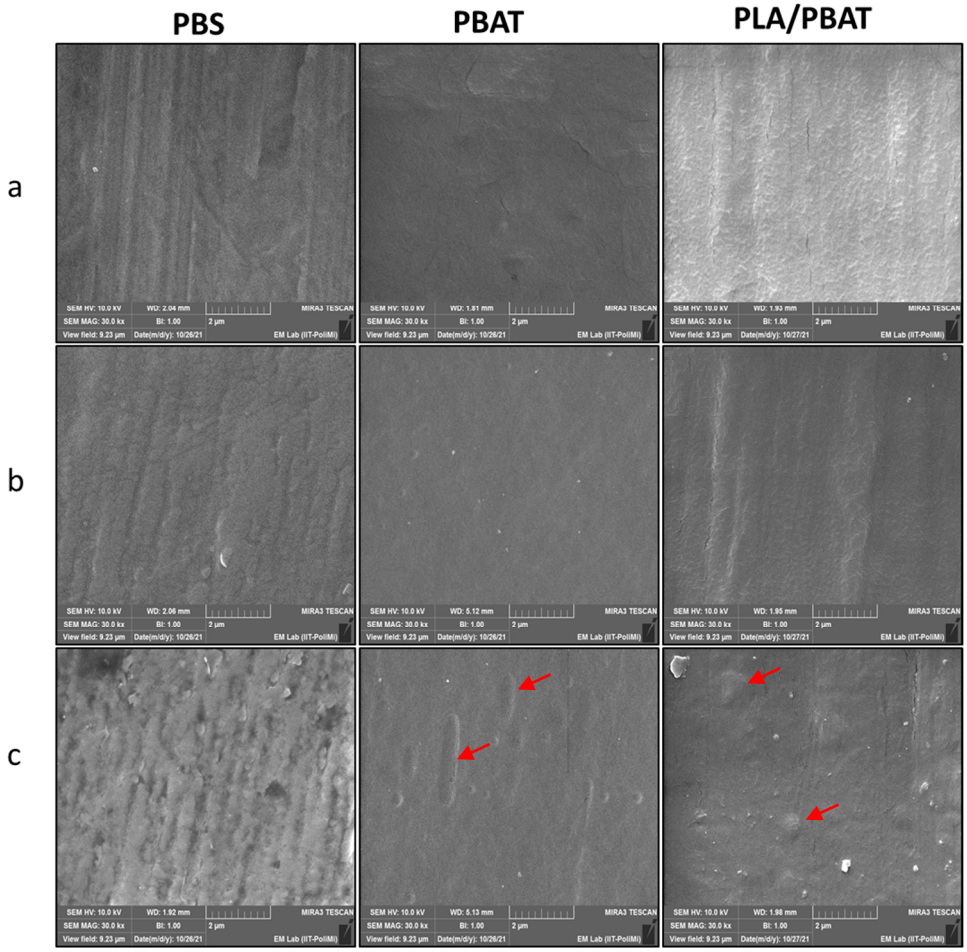

Figure 3. SEM images of PBS, PBAT and PLA/PBAT blend in their untreated state (**a**) and treated with 1 min (**b**) and 2 min (**c**) Ar post-crosslinking process. A few defects are identified in the figures by red arrows.

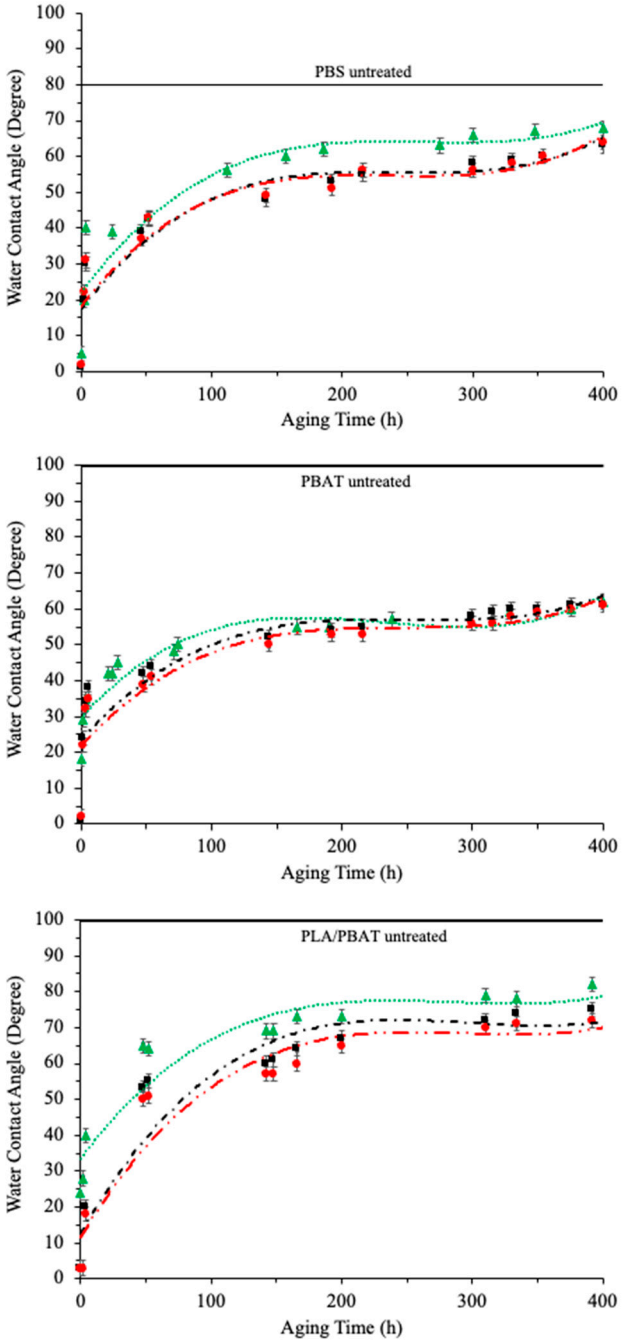

Figure 4. WCA value of PBS, PBAT and PLA/PBAT blend after pure O_2 plasma treatment of 30 s (green curve), and oxygen with Ar post-crosslinking treatment of 1 min (black curve) and 2 min (red curve) during 15 days of ageing time.

3.4. FTIR Characterization

For clarity, in Figure 5 are presented FTIR spectra of the pristine BPs versus those treated with the 1 min Ar post-crosslinking process. The untreated PBS spectrum is characterized by the general functional groups of its polymer chain structure [37]: the peak at about 2920 cm^{-1} corresponds to C-H stretching mode of methylene groups; the prominent peak at about 1720 cm^{-1} is due to the C=O vibration of carboxyl groups, the C-O ester group vibration peak at about 1332 cm^{-1} and the prominent C=O carbonyl group vibration peak at about 1160 cm^{-1}. Regarding the untreated PBAT spectrum, peaks between 2800 and 2900 cm^{-1} represent the asymmetric and symmetric stretching vibration of the successive methylene groups present in the adipate unit and 1,4 butanediol unit [38,39].

The peak at about 1710 cm^{-1} is due to the C=O stretching mode of carbonyl functional groups [40], while C-O stretching vibrations are highlighted by a 1260 cm^{-1} peak. The presence of a phenyl ring in the PBAT structure is confirmed by 870 cm^{-1} and 730 cm^{-1} peaks which are due to the out-of-plane bending vibration of this structure [41]. The peaks at about 1170 cm^{-1} and 1100 cm^{-1} are characteristic of adipate and terephthalate fractions in the BP structure. It is also noteworthy that the presence of a transmission peak at 3400 cm^{-1} is related to the -OH stretching mode of the benzyl alcohol unit. Finally, in the untreated blend spectrum, there are the characteristic peaks of the PBAT just mentioned, while the presence of PLA is evidenced by the appearance of different typical peaks at 1750 cm^{-1}, 1180–1086 cm^{-1} and 3000 cm^{-1} caused by the stretching of C=O, C-O and C-H chemical bonds, respectively [42].

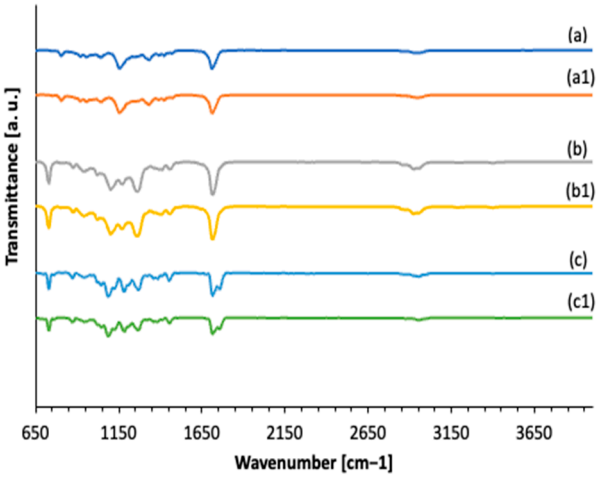

Figure 5. FTIR spectra of native PBS (a), PBAT (b) and PLA/PBAT blend (c) and treated PBS (a1), PBAT (b1) and PLA/PBAT (c1).

As shown in Figure 5, for all treated BPs, the plasma process does not produce the formation of any new chemical functional group on the surface, highlighting how these treatments are not invasive, but for the sake of completeness, it should be noted that FTIR in this case is used as a bulk analysis methodology; therefore, the measurements reported in Figure 5 refer to the typical depth of penetration in ATR ranges from several hundred nanometers to several microns [43]. It is, however, possible to extract qualitative information in nanometric layers from the IR characterization through the IR band ratio comparison [44] before and immediately after plasma treatments (Figure 6), using the integrated area of wavenumber ranges. This could be due to the fact that the internal reflections enhance the sensitivity of the ATR accessory toward components in low concentrations [45,46]. Oxidation driven by plasma could promote C-H bond-breaking phenomena which lead to an increase in C-O and C=O in the BP structure. This oxidation process is responsible for changing the wettability and adhesion of samples once they are treated with plasma.

As shown in Figure 6, all treated samples are characterized by a decreasing C-H band intensity and the presence of much more oxygen functional groups. In particular, plasma treatment enhances the breaking of C-H bonds, favoring the formation of C=O and C-O functional groups on the sample surface. This functionalization phenomenon causes the hydrophilicity behavior of BPs and it is confirmed by the WCA value decreasing after this kind of activation (Figure 4). Moreover, plasma treatments that functionalize polymer surfaces with hydrophilic groups, apart from decreasing the contact angle, concurrently result in an increase in surface energy, particularly in the polar component [47]. This can positively impact the adhesion of inks and labels and the sealing properties of the material.

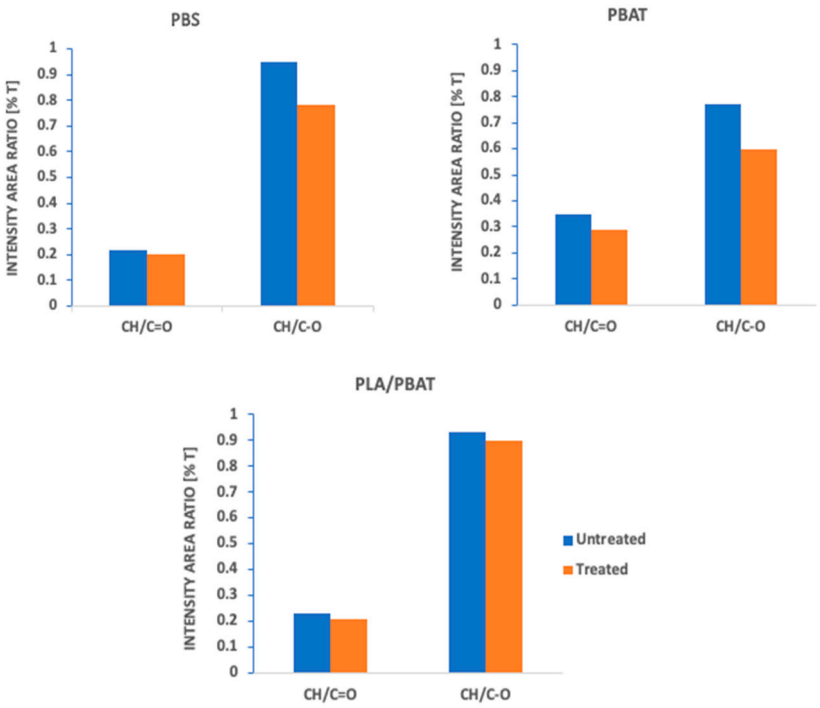

Figure 6. IR band ratio comparison between untreated and activated BPs immediately after plasma treatment.

3.5. XRD Analysis

In order to find deviations from the bulk properties, X-ray diffraction analysis was performed on untreated and treated samples (oxygen and Ar post-crosslinking treatment of 1 min) by collecting and comparing the corresponding XRD spectra (Figure 7). PBS is a semi-crystalline polymer (Figure 7a). The X-ray diffraction peaks at 2θ = 19.7°, 22.6°, 22.8°, 26.1° and 28.6°, corresponding to the (020), (110), (121) and (111) planes of the PBS, are clearly visible [48] and the calculated degree of crystallinity is ~77%. Any significant change has resulted in showing an unchanged crystallinity state after the plasma treatment. Regarding the PBAT and PLA/PBAT blend samples, the patterns have very broad features and low intensity, consistent with amorphous solids. The characteristic peaks of PBAT could be assigned to (011), (010), (110) and (100) planes for 2θ values between 15° and 30° (also (111) peak in the PBAT sample) [49,50]. Also, in this case, we can say that the plasma treatment did not produce changes in the treated PBAT sample with respect to the untreated one. In the treated PLA/PBAT blend sample, a small change is detectable regarding the unclear presence of the (010) peak; nonetheless, we consider this change not substantial.

3.6. DSC Analysis

Figure 8 reports the DSC thermograms obtained for the three systems investigated to compare the thermal properties of the untreated material (as reference) to the plasma-treated ones (oxygen and Ar post-crosslinking treatment of 1 min) over the 15 days, i.e., the ready-to-use materials for industrial applications. Aiming at assessing the behavior of the actual ready-to-use materials, the first heating runs were compared without subjecting the samples to any previous thermal treatment. The observed endothermic and exothermic signals reflect the typical transitions (glass transition, crystallization and melting) displayed by these polymers over the temperature range investigated, which are already widely described in the literature [35,51,52]. A detailed characterization of the specific behavior of such polymers is beyond the scope of this analysis, which is focused on the effects derived from the plasma treatment. It suffices here to highlight that the comparison of the

thermograms of the reference and the plasma-treated samples reveals an almost perfect superimposition of the traces, suggesting that the polymer bulk properties are not affected by the treatment, and that their stability properties are fully comparable to the respective reference system ones.

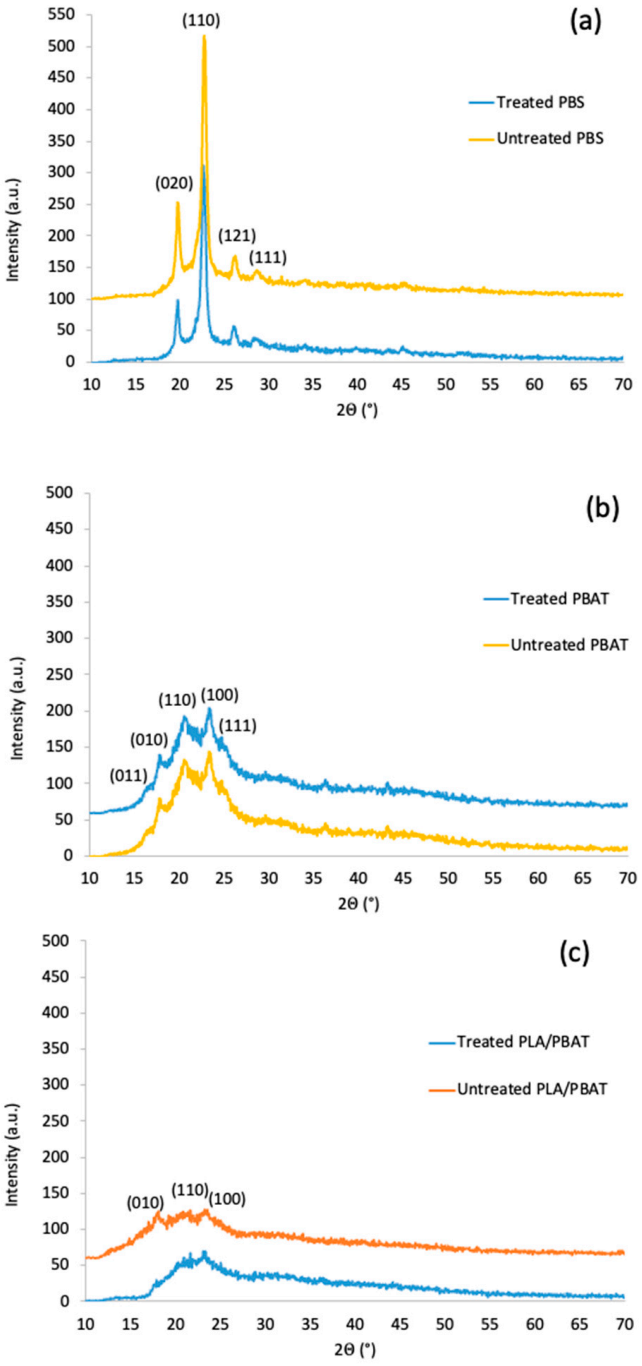

Figure 7. XRD spectra of untreated and plasma-treated (**a**) PBS, (**b**) PBAT and (**c**) PLA/PBAT blend samples.

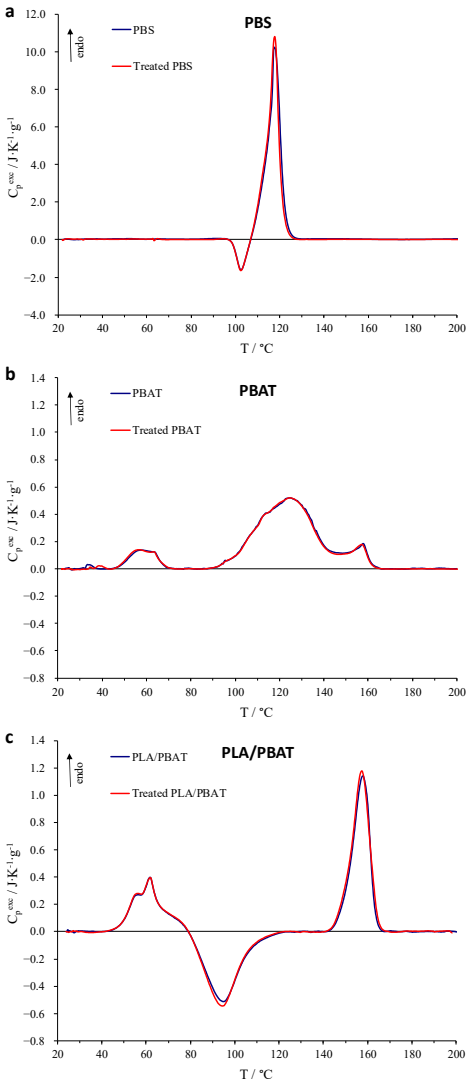

Figure 8. DSC heating scan thermograms (5 °C/min scanning rate) of untreated (blue trace) and plasma-treated (red trace) (**a**) PBS, (**b**) PBAT and (**c**) PLA/PBAT blend samples.

4. Conclusions

Enhancing the surface energy of plastics for adhesives, inks, paint and metallization processes is always a crucial topic in different industrial applications. Although a high wettability is easily achieved, for example, through plasma treatment, the loss of this effect (hydrophobic recovery) is equally fast. It is therefore essential to study processes to minimize this effect. The hydrophobic recovery of commercial plastics (derived from petroleum hydrocarbons) after an activation treatment by plasma has been reported by various authors. Regarding biodegradable plastics and particularly those used in food, the scientific literature specifically focused on this effect is quite poor. For that purpose, in this experimental work, the wettability of various biodegradable plastics (PBS, PBAT and a PLA/PBAT blend) was enhanced by a low-pressure plasma treatment. The used process parameters were derived from a previous study of ours [28], in which we had demonstrated that an appropriate plasma treatment (first, a few seconds of oxygen plasma for activation, then an Ar plasma for crosslinking) was optimal to slow down = hydrophobic recovery. In this paper, this phenomenon has been analyzed through the variation in crosslinking time. Given that crosslinking times lower than 1 min (30 and 45 s) gave very similar results (or not significantly better) to the case with only oxygen, the experimental work has been addressed to times equal to or larger than 1 min. Based on the obtained results of ageing

(intended as hydrophobic recovery) within a period of 15 days, the plasma treatment of 30 s of oxygen with 1 min of Ar post-treatment appears to be the optimal treatment for PBS, PBAT and PLA/PBAT functionalization. The weight loss due to the plasma process was analyzed. As expected, the use of oxygen during plasma activation results in greater weight loss compared to modification with argon. However, in the process used, the total etching rate seems very low. Using the latter process, regarding the bulk properties, XRD and DSC analyses revealed no bulk modification of the BPs. The FTIR also confirmed that the plasma treatment is not invasive and only a surface effect (oxidation with changes in wettability) is produced.

Author Contributions: E.V. conceptualization, supervision, project administration, funding acquisition and writing—original draft; M.A. conceptualization, methodology, writing—original draft and investigation; M.P. conceptualization, methodology, writing—original draft, investigation and writing—review and editing; S.M.P. resources, investigation, and review and editing; R.D. resources, investigation, and review and editing; F.S. resources, investigation, and review editing; D.F. resources, investigation, and review and editing. All authors have read and agreed to the published version of the manuscript.

Funding: This research was funded by the sPATIALS3 project (ID 1176485). It was financed by the European Regional Development Fund under the ROP of the Lombardy Region ERDF 2014-2020—Axis I "Strengthen technological research, development and innovation and Action 1. b.1.3 "Support for co-operative R&D activities to develop new sustainable technologies, products and services"—Call Hub.

Institutional Review Board Statement: Not applicable.

Informed Consent Statement: Not applicable.

Data Availability Statement: The data presented in this study are available on request from the corresponding author. The data are not publicly available due to privacy.

Acknowledgments: The authors acknowledge Davide Della Torre of the CNR-ICMATE for his helpful technical assistance in the setup of the X-ray diffraction instrumentation. The authors wish to thank Corapack Srl (Brenna (CO), Italy) for providing BioPBS™ FZ91PM/FZ91PB, PBAT and PLA/PBAT substrates.

Conflicts of Interest: The authors declare no conflicts of interest.

References

1. Adeyeye, O.A.; Sadiku, E.R.; Reddy, A.B.; Ndamase, A.S.; Makgatho, G.; Sellamuthu, P.S.; Perumal, A.B.; Nambiar, R.B.; Fasiku, V.O.; Ibrahim, I.D.; et al. The use of biopolymers in food packaging. In *Green Biopolymers and Their Nanocomposites*; Gnanasekaran, D., Ed.; Springer: Singapore, 2019; pp. 137–158. [CrossRef]
2. North, E.J.; Halden, R.U. Plastics and environmental health: The road ahead. *Rev. Environ. Health* **2013**, *28*, 1–8. [CrossRef]
3. Pellicer, E.; Nikolic, D.; Sort, J.; Baró, M.; Zivic, F.; Grujovic, N.; Grujic, R.; Pelemis, S. *Advances in Applications of Industrial Biomaterials*; Springer Science and Business Media LLC: Dordrecht, The Netherlands, 2017; ISBN 9783319627663.
4. Meiron, T.; Saguy, I. Wetting properties of food packaging. *Food Res. Int.* **2007**, *40*, 653–659. [CrossRef]
5. Nemani, S.K.; Annavarapu, R.K.; Mohammadian, B.; Raiyan, A.; Heil, J.; Haque, M.A.; Abdelaal, A.; Sojoudi, H. Surface Modification of Polymers: Methods and Applications. *Adv. Mater. Interfaces* **2018**, *5*, 1801247. [CrossRef]
6. Sheng, E.; Sutherland, I.; Brewis, D.; Heath, R. Effects of the chromic acid etching on propylene polymer surfaces. *J. Adhes. Sci. Technol.* **1995**, *9*, 47–60. [CrossRef]
7. Drobota, M.; Gradinaru, L.M.; Ciobanu, C.; Vasilescu, D.S. Effect of chemical treatment of poly(ethylene terephthalate) surfaces on mechanical and water-sorption properties. *Univ. Politeh. Buchar. Sci. Bull. Ser. B-Chem. Mater. Sci.* **2015**, *77*, 131–140.
8. Hambardzumyan, A.; Biltresse, S.; Dufrêne, Y.; Marchand-Brynaert, J. An Unprecedented Surface Oxidation of Polystyrene Substrates by Wet Chemistry under Basic Conditions. *J. Colloid Interface Sci.* **2002**, *252*, 443–449. [CrossRef] [PubMed]
9. Zhou, J.; Ellis, A.V.; Voelcker, N.H. Recent developments in PDMS surface modification for microfluidic devices. *Electrophoresis* **2010**, *31*, 2–16. [CrossRef] [PubMed]
10. Desmet, T.; Morent, R.; De Geyter, N.; Leys, C.; Schacht, E.; Dubruel, P. Nonthermal Plasma Technology as a Versatile Strategy for Polymeric Biomaterials Surface Modification: A Review. *Biomacromolecules* **2009**, *10*, 2351–2378. [CrossRef] [PubMed]
11. Bahrami, R.; Zibaei, R.; Hashami, Z.; Hasanvand, S.; Garavand, F.; Rouhi, M.; Jafari, S.M.; Mohammadi, R. Modification and improvement of biodegradable packaging films by cold plasma; a critical review. *Crit. Rev. Food Sci. Nutr.* **2020**, *62*, 1936–1950. [CrossRef] [PubMed]

12. Praveen, K.M.; Pious, C.V.; Thomas, S.; Grohens, Y. *Non-Thermal Plasma Technology for Polymeric Materials: Applications in Composites, Nanostructured Materials, and Biomedical Fields*; Mozetič, M., Špatenka, P., Praveen, K.M., Thomas, S., Cvelbar, U., Eds.; Elsevier: Amsterdam, The Netherlands, 2019.
13. Hsu, S.-H.; Chen, K.-S.; Lin, H.-R.; Chang, S.-J.; Tang, T.-P. Effect of Plasma Gas Flow Direction on Hydrophilicity of Polymer by Small Zone Cold Plasma Treatment and Hydrophobic Plasma Treatment. *Int. J. Distrib. Sens. Netw.* **2009**, *5*, 429–436. [CrossRef]
14. Ataeefard, M.; Moradian, S.; Mirabedini, M.; Ebrahimi, M.; Asiaban, S. Investigating the effect of power/time in the wettability of Ar and O2 gas plasma-treated low-density polyethylene. *Prog. Org. Coat.* **2009**, *64*, 482–488. [CrossRef]
15. Kostov, K.; Nishime, T.; Castro, A.; Toth, A.; Hein, L. Surface modification of polymeric materials by cold atmospheric plasma jet. *Appl. Surf. Sci.* **2014**, *314*, 367–375. [CrossRef]
16. Masruroh; Santjojo, D.J.D.H. Surface modification of polystyrene by nitrogen plasma treatment. In *Coatings and Thin-Film Technologies*; Perez-Taborda, J.A., Bernal, A.G.A., Eds.; IntechOpen: London, UK, 2019. [CrossRef]
17. Slepička, P.; Trostová, S.; Kasálková, N.S.; Kolská, Z.; Sajdl, P.; Švorčík, V. Surface Modification of Biopolymers by Argon Plasma and Thermal Treatment. *Plasma Process. Polym.* **2011**, *9*, 197–206. [CrossRef]
18. Mohammadalipour, M.; Asadolahi, M.; Mohammadalipour, Z.; Behzad, T.; Karbasi, S. Plasma surface modification of electrospun polyhydroxybutyrate (PHB) nanofibers to investigate their performance in bone tissue engineering. *Int. J. Biol. Macromol.* **2023**, *230*, 123167. [CrossRef]
19. Fu, S.; Zhang, P. Surface modification of polylactic acid (PLA) and polyglycolic acid (PGA) monofilaments via the cold plasma method for acupoint catgut-embedding therapy applications. *Text. Res. J.* **2019**, *89*, 3839–3849. [CrossRef]
20. Licciardello, M.; Ciardelli, G.; Tonda-Turo, C. Biocompatible Electrospun Polycaprolactone-Polyaniline Scaffold Treated with Atmospheric Plasma to Improve Hydrophilicity. *Bioengineering* **2021**, *8*, 24. [CrossRef]
21. Bhushan, B.; Kumar, R. Plasma Treated and Untreated Thermoplastic Biopolymers/Biocomposites in Tissue Engineering and Biodegradable Implants. In *Materials for Biomedical Engineering*; Elsevier: Amsterdam, The Netherlands, 2019; pp. 339–369, ISBN 978-0-12-816901-8.
22. Wei, Z.; Gu, J.; Ye, Y.; Fang, M.; Lang, J.; Yang, D.; Pan, Z. Biodegradable poly(butylene succinate) nanofibrous membrane treated with oxygen plasma for superhydrophilicity. *Surf. Coat. Technol.* **2019**, *381*, 125147. [CrossRef]
23. Bélard, L.; Poncin-Epaillard, F.; Dole, P.; Avérous, L. Plasma-polymer coatings onto different biodegradable polyesters surfaces. *Eur. Polym. J.* **2013**, *49*, 882–892. [CrossRef]
24. Zhang, R.; Lan, W.; Ding, J.; Ahmed, S.; Qin, W.; He, L.; Liu, Y. Effect of PLA/PBAT Antibacterial Film on Storage Quality of Passion Fruit during the Shelf-Life. *Molecules* **2019**, *24*, 3378. [CrossRef] [PubMed]
25. Che, C.; Dashtbozorg, B.; Li, X.; Dong, H.; Jenkins, M. Effect of μPlasma Modification on the Wettability and the Ageing Behaviour of Glass Fibre Reinforced Polyamide 6 (GFPA6). *Materials* **2021**, *14*, 7721. [CrossRef]
26. Kim, B.K.; Kim, K.S.; Park, C.E.; Ryu, C.M. Improvement of wettability and reduction of aging effect by plasma treatment of low-density polyethylene with argon and oxygen mixtures. *J. Adhes. Sci. Technol.* **2002**, *16*, 509–521. [CrossRef]
27. Vassallo, E.; Aloisio, M.; Pedroni, M.; Ghezzi, F.; Cerruti, P.; Donnini, R. Effect of Low-Pressure Plasma Treatment on the Surface Wettability of Poly(butylene succinate) Films. *Coatings* **2022**, *12*, 220. [CrossRef]
28. Vassallo, E.; Pedroni, M.; Silvetti, T.; Morandi, S.; Brasca, M. Inactivation of *Staphylococcus aureus* by the synergistic action of charged and reactive plasma particles. *Plasma Sci. Technol.* **2020**, *22*, 085504. [CrossRef]
29. Chung, P.M.; Talbot, L.; Touryan, K.J. *Electric Probes in Stationary and Flowing Plasma*; Springer: New York, NY, USA, 1975.
30. Chen, F.F. *Plasma Diagnostic Techniques*; Huddlestone, R.H., Leonard, S.L., Eds.; Academic Press: Cambridge, MA, USA, 1965; p. 113.
31. Heidenreich, J.E.; Paraszczak, J.R.; Moisan, M.; Sauve, G. Electrostatic probe analysis of microwave plasmas used for polymer etching. *J. Vac. Sci. Technol. B Microelectron. Nanometer Struct.* **1987**, *5*, 347–354. [CrossRef]
32. Harrick, N.J.; du Pré, F.K. Effective Thickness of Bulk Materials and of Thin Films for Internal Reflection Spectroscopy. *Appl. Opt.* **1966**, *5*, 1739–1743. [CrossRef]
33. Vafaei, N.; Ribeiro, R.A.; Camarinha-Matos, L.M. Normalization techniques for multi-criteria decision making: Analytical hierarchy process case study. In Proceedings of the Doctoral Conference on Computing, Electrical and Industrial Systems, Costa de Caparica, Portugal, 11–13 April 2016; pp. 261–269.
34. Puliyalil, H.; Cvelbar, U. Selective Plasma Etching of Polymeric Substrates for Advanced Applications. *Nanomaterials* **2016**, *6*, 108. [CrossRef]
35. Su, S.; Duhme, M.; Kopitzky, R. Uncompatibilized PBAT/PLA Blends: Manufacturability, Miscibility and Properties. *Materials* **2020**, *13*, 4897. [CrossRef]
36. Borcia, C.; Punga, I.; Borcia, G. Surface properties and hydrophobic recovery of polymers treated by atmospheric-pressure plasma. *Appl. Surf. Sci.* **2014**, *317*, 103–110. [CrossRef]
37. Aziman, N.; Kian, L.K.; Jawaid, M.; Sanny, M.; Alamery, S. Morphological, Structural, Thermal, Permeability, and Antimicrobial Activity of PBS and PBS/TPS Films Incorporated with Biomaster-Silver for Food Packaging Application. *Polymers* **2021**, *13*, 391. [CrossRef]
38. Sim, J.Y.; Raj, C.J.; Yu, K.H. Poly(butylene adipate-co-terephthalate) (PBAT)/Antimony-doped Tin Oxide Polymer Composite for Near Infrared Absorption Coating Applications. *Bull. Korean Chem. Soc.* **2019**, *40*, 674–679. [CrossRef]

39. Pokhrel, S.; Sigdel, A.; Lach, R.; Slouf, M.; Sirc, J.; Katiyar, V.; Bhattarai, D.R.; Adhikari, R. Starch-based biodegradable film with poly(butylene adipate-*co*-terephthalate): Preparation, morphology, thermal and biodegradation properties. *J. Macromol. Sci. Part A* **2021**, *58*, 610–621. [CrossRef]
40. De Matos Costa, A.R.; Crocitti, A.; de Carvalho, L.H.; Carroccio, S.C.; Cerruti, P.; Santagata, G. Properties of Biodegradable Films Based on Poly(butylene Succinate) (PBS) and Poly(butylene Adipate-*co*-Terephthalate) (PBAT) Blends. *Polymers* **2020**, *12*, 2317. [CrossRef]
41. Nobile, M.R.; Crocitti, A.; Malinconico, M.; Santagata, G.; Cerruti, P. Preparation and characterization of polybutylene succinate (PBS) and polybutylene adipate-terephthalate (PBAT) biodegradable blends. In Proceedings of the 9th International Conference on "Times of Polymers and Composites": From Aerospace to Nanotechnology, Naples, Italy, 17–21 June 2018; p. 020180.
42. Jordá-Vilaplana, A.; Fombuena, V.; García-García, D.; Samper, M.D.; Sánchez-Nácher, L. Surface modification of polylactic acid (PLA) by air atmospheric plasma treatment. *Eur. Polym. J.* **2014**, *58*, 23–33. [CrossRef]
43. Harrick, N.J. Study of Physics and Chemistry of Surfaces from Frustrated Total Internal Reflections. *Phys. Rev. Lett.* **1960**, *4*, 224–226. [CrossRef]
44. Almond, J.; Sugumaar, P.; Wenzel, M.N.; Hill, G.; Wallis, C. Determination of the carbonyl index of polyethylene and polypropylene using specified area under band methodology with ATR-FTIR spectroscopy. *e-Polymers* **2020**, *20*, 369–381. [CrossRef]
45. Harrick, J. *Internal Reflection Spectroscopy*; Interscience: New York, NY, USA, 1975.
46. De Geyter, N.; Morent, R.; Leys, C. Surface characterization of plasma-modified polyethylene by contact angle experiments and ATR-FTIR spectroscopy. *Surf. Interface Anal.* **2007**, *40*, 608–611. [CrossRef]
47. Chen, G.; Dong, S.; Zhao, S.; Li, S.; Chen, Y. Improving functional properties of zein film via compositing with chitosan and cold plasma treatment. *Ind. Crop. Prod.* **2019**, *129*, 318–326. [CrossRef]
48. Xu, J.; Guo, B.-H. Microbial succinic acid, its polymer Poly(butylene succinate), and applications. In *Plastics from Bacteria*; Chen, G.Q., Ed.; Springer: Berlin/Heidelberg, Germany, 2009; pp. 347–388. [CrossRef]
49. Wang, X.; Cui, L.; Fan, S.; Li, X.; Liu, Y. Biodegradable Poly(butylene adipate-*co*-terephthalate) Antibacterial Nanocomposites Reinforced with MgO Nanoparticles. *Polymers* **2021**, *13*, 507. [CrossRef]
50. Da Silva, C.G.; Kano, F.S.; Rosa, D.S. Lignocellulosic Nanofiber from Eucalyptus Waste by a Green Process and Their Influence in Bionanocomposites. *Waste Biomass Valorization* **2019**, *11*, 3761–3774. [CrossRef]
51. Park, J.W.; Im, S.S. Phase behavior and morphology in blends of poly(L-lactic acid) and poly(butylene succinate). *J. Appl. Polym. Sci.* **2002**, *86*, 647–655. [CrossRef]
52. Yoo, E.S.; IM, S.S. Melting Behavior of Poly(butylene succinate) during Heating Scan by DSC. *J. Polym. Sci. Part B Polym. Phys.* **1999**, *37*, 1357–1366. [CrossRef]